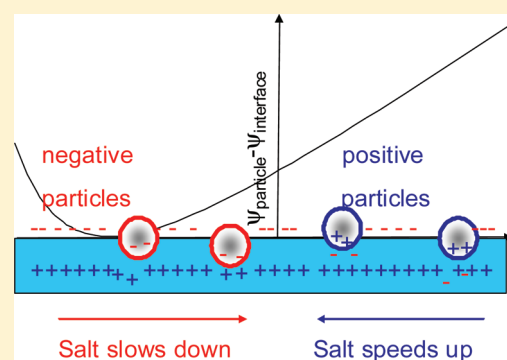


# Diffusion of Nanoparticles at an Air/Water Interface Is Not Invariant under a Reversal of the Particle Charge

T. Gehring and Th. M. Fischer\*

Institute of Experimental Physics V, The University of Bayreuth, 95440 Bayreuth, Germany

**ABSTRACT:** The diffusion of charged nanoparticles at an aqueous/air interface is not invariant under a charge reversal of the particles. Negatively charged particles slow down with the ionic strength of the aqueous phase, while positively charged particles speed up. The diffusion constant of the particles reflects their immersion into the aqueous/air interface. We argue that the opposing behavior of oppositely charged particles is proof that the immersion depth of the particles scales with the contrast in electric surface potential of the particle to the electric surface potential of the air/water interface, not with the particle's charge density. We therefore propose to incorporate the potential drop across the air/water interface into theories of electro-dipping.



## INTRODUCTION

Mesoscopic particles residing at an interface that are smaller than the capillary length appear to be force free since gravitational forces become negligible. Their immersion can be well described by a balance of interfacial tensions at the three-phase contact line and by the trivial flat solution to the Young Laplace equation in a gravitation free nonelectric environment. For nanoscopic particles the Debye length becomes comparable to the size of the particles and electrostatic forces need to be considered. Nikolaides and co-workers<sup>1</sup> proposed that charged particles should be pressed into the air/water interface, because the electric field energy caused by the surface charges on the particles can be minimized by shielding it with counterions, the deeper the particles are immersed into the interface. The lowering of electrostatic field energy, however, costs surface energy because the air/water interface must be deformed. The pressure balance between electrostatic and capillary pressure on the particle and the aqueous/air interface then decides the actual position of the particle in a similar way gravitational and capillary effects are deciding the position of larger particles.

The model of Nikolaides has been criticized, because it also predicted to cause a long-range electrocapillary interaction. Megens and Aizenberg<sup>2</sup> showed that the overlap of capillary deformations is negligible and cannot lead to long-range electrocapillary interactions between the particles, because contrary to the predictions of Nikolaides the interaction is of short range. Megens and Aizenberg did not, however, argue on the existence of a dipping force. Later work by Oettel and Dietrich<sup>3</sup> theoretically also showed that the dipping effect should be relatively weak, because the dipole density of the double layer has negligible drop of electrostatic potential. In the latter theoretical treatment, however, electrostatic effects at the aqueous/air interface have been neglected and the aqueous/air interface has been treated as free of surface potential.

The aqueous/air interface carries a surface potential<sup>4</sup> of the order of  $-50$  mV due to a surface excess of  $\text{OH}^-$  ions in the topmost water layer and a depletion of  $\text{H}_3\text{O}^+$ . The surface potential of the aqueous/air interface manifests itself by the electrophoretic motion of air bubbles.<sup>5</sup> It is of similar magnitude as typical surface potentials of charged nanoparticles. In previous work,<sup>6</sup> we have shown that electrostatics does play a role for the mobility of nanoparticles at the air–water interface. The purpose of the present work is to experimentally test whether there is also evidence for the influence of the surface potential of water on the particle mobility.

One fundamental law in physics is the invariance of classical phenomena under charge reversal. On the basis of this law, one would expect the mobility of a particle at the air/water interface to be invariant under a full charge reversal of the system. For a particle of opposite charge, co-ions and counterions interchange their roles and since the mobilities of both the co-ions and the counterions are orders of magnitude larger than the mobility of the nanoparticle, all ions can be considered quasistatic. Therefore, differences in mobilities of anions and cations should be irrelevant for the mobility of the particle. An apparent violation of the charge reversal invariance therefore is evidence for an incomplete charge reversal. In the current article, we will show that the mobility of positive and negative nanoparticles changes in a different way with the ionic strength of the aqueous phase. We interpret this as an incomplete charge reversal and argue that this proves the importance of the electric dipolar nature of the air/water interface that does not reverse sign as we change the charge of the nanoparticles.

Received: June 30, 2011

Revised: September 22, 2011

Published: November 02, 2011

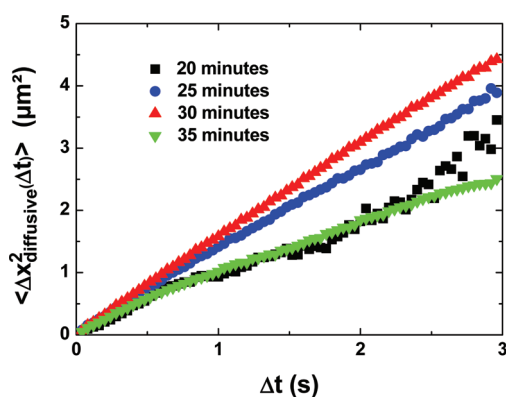


**Figure 1.** Diffusive mean square displacement of amine-modified polystyrene nanoparticles on a sodium chloride/air interface with an ionic strength of  $10^{-5}$  M as a function of time. The data of each curve was collected 20, 25, 30, and 35 min after the particle/methanol solution was spread on the surface.

## EXPERIMENTAL SECTION

We use particle tracking methods to follow the motion of nanoparticles at an aqueous/air interface to measure the mobility of individual particles as a function of ionic strength. We use fluorescent amine-modified particles of diameter  $2a = 190$  nm purchased from Invitrogen (Invitrogen FluoSpheres F8763 amine-modified microspheres), as well as carboxylate-modified particles of a diameter 100 nm (Invitrogen FluoSpheres F8801 carboxylate-modified microspheres), dispersed in an aqueous solution. Interfacial diffusion of nanoparticles is dominated by their immersion into the aqueous phase and by surface rheological effects<sup>7–9</sup> caused here by surfactant impurities released from the nanoparticles. Care therefore was taken to minimize the effects of surfactant impurities. We always followed the same cleaning procedure to ensure comparable results. At the beginning, drops of the purchased aqueous particle solution were poured into a stock solution stored in a snap-cap vial.

By use of a Hamilton syringe,  $0.2 \mu\text{L}$  of the particle solution was injected into 3 mL of Nanopure water (Siemens SG-LaboStar 7 TWF-DI Ultrapure water system of resistivity of  $18 \text{ M}\Omega \text{ cm}^{-1}$ ). By use of a Tube-O-dialyzer, this diluted solution was dialyzed in a beaker glass containing 50 mL of methanol. After dialysis, the particle solution, now dissolved in methanol, was immediately transferred into a glass snap-cap vial. Particles were then spread from this methanol solution onto the air/water interface. The experiments were performed in a special made 3 cm tall Petri dish. Experiments were performed with methanol solutions not older than 2 days after preparation of the solution. No ion exchangers<sup>10</sup> were used to clean the particles. All glass jars used during preparation of the experiment were purged with chloroform followed by numerous flushings with Nanopure water. To complete the cleaning, we heated the glass jars 5–10 min using a Bunsen burner. Pipets and syringes were soaked three times with chloroform and 10 times with water.

A top cover on the Petri dish with a hole for the microscope's objective minimized convection of the air above the air/water surface. The diffusion processes were monitored and recorded using a fluorescence microscope with a CCD camera attached to it with a resolution of  $1392 \times 1040$  pixels and a frame rate of 25 Hz. The entire setup was placed on an antivibration table. We used a  $63\times$  objective of the microscope leading to a resolution of

$0.1 \mu\text{m}/\text{pixel}$  that proved to be a good compromise between resolution and the field of view. A smaller field of view results in fewer beads that can be followed simultaneously and a reduced statistics. We worked with particle surface concentrations of  $10^{-3}$  beads per  $\mu\text{m}^2$  to suppress effects of static particle–particle and hydrodynamic interactions. Nevertheless, we observed regions where particles aggregated into clusters of higher density. Such particles were eliminated later by the evaluation software.

Every experiment started with filling 3 mL of Nanopure water into a Petri dish. After addition of different amounts of sodium chloride, obtained from Fisher Scientific and claimed to be  $>99\%$  pure,  $20 \mu\text{L}$  of the particle/methanol solution was spread on the surface. Sonication of the colloidal methanol solution for 1 h before spreading ensured a good homogeneous dispersion on the surface. Experiments were started 20 min after the particle solution was spread. Videos of the particle motion were recorded over a duration of 20 min and stored on the computer.

## EVALUATION

Each video was split into four sequences covering the time 20, 25, 30, and 35 min after the particle/methanol solution was applied. To determine the mean square displacement, the video sequences were fragmented into image sequences that were then analyzed using particle-tracking routines written by us in Matlab. Particles were accepted as proper particles if their gray value caused by the fluorescence intensity fell in the proper window, and if their sizes fell into the proper range.

The motion of the particle is a result of its diffusion and a superposed drift of the entire surface caused by convective flow of the air above the surface. The convection varies only on much larger scales than the field of view. The two-dimensional vector displacement of the particles by convection can therefore be computed as the average displacement of all  $N_t$  particles visible from one frame to the next:

$$\Delta \mathbf{x}_{\text{drift}}(t, t-1) = \frac{\sum_j^{N_t} \mathbf{x}_j(t) - \mathbf{x}_j(t-1)}{N_t} \quad (1)$$

Here  $\mathbf{x}_j(t) - \mathbf{x}_j(t-1)$  denotes the displacement of particle  $j$  from one frame to the next. The drift displacement after several frames is just the sum over the drift displacements between two consecutive frames:

$$\Delta \mathbf{x}_{\text{drift}}(t, t-\Delta t) = \sum_{fr=0}^{\Delta t-1} \Delta \mathbf{x}_{\text{drift}}(t-\Delta t + fr + 1, t-\Delta t + fr) \quad (2)$$

The diffusive mean square displacement is the mean square displacement where drift effects have been subtracted:

$$\langle \Delta \mathbf{x}_{\text{diffusive}}^2(\Delta t) \rangle = \frac{1}{N(\Delta t)} \sum_{i,t} [\mathbf{x}_i(t) - \mathbf{x}_i(t-\Delta t) - \Delta \mathbf{x}_{\text{drift}}(t, t-\Delta t)]^2 \quad (3)$$

where  $N(\Delta t)$  is the event number, i.e., the number of times where the same particles are observed in images separated by a period of  $\Delta t$ . Figure 1 shows the diffusive mean square displacement of the nanoparticles as a function of the time lag  $\Delta t$ . In each experiment the four video sequences usually show varying diffusion constants with different slopes. Slopes have been fitted to the short

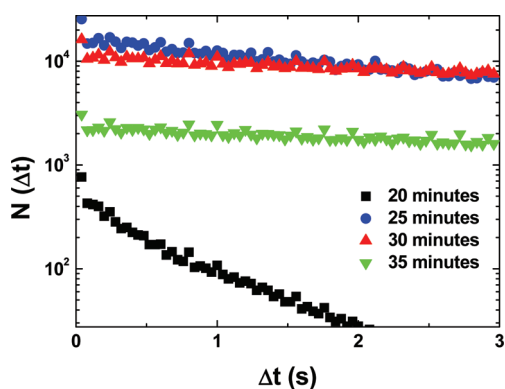


**Figure 2.** Number of events contributing to the mean square displacement at different times. The data corresponds to the mean square displacement data of figure 1.

time behavior  $\Delta t < 0.5$  s. The scatter of the data occurs due to subdiffusive behavior, which is caused by particle–particle interactions. Especially when particles diffuse over longer times, they might come into the range of other particles, causing the slope to decrease with time as seen in the 20 and 35 min data in Figure 1. Discrimination between particles that are free to diffuse and those forming an aggregated cluster is not complete in our software, such that systematic underestimation of the individual diffusion of particles occurred, especially when particles binding to rigid clusters have been overlooked by the software. Data was therefore checked via eye inspection by examining the original video of particles. Erasing those clusters from the analysis brought back the slope of the long time mean square displacement to the short time slope that remained unaltered by the erasure. Whenever clusters were too frequent, the data was discarded. Typical data of one video sequence showed values of the event number  $N(\Delta t)$  ranging from  $1000 < N(\Delta t) < 10000$  for lag times below  $\Delta t < 1$  s (Figure 2). A large number of events results in negligible statistical error of the computed diffusive mean square displacement and the diffusion constant ( $\Delta D/D \approx 10^{-2}$ ). This can be seen in Figures 1 and 2. The data at 25, 30, and 35 min after spreading in Figure 2 show a reasonable amount of events, while the number of events are 1–2 orders of magnitude lower for the data at 20 min. The corresponding diffusive mean square displacement in Figure 1 is smooth for the 25, 30, and 35 min data, while it exhibits significant scatter for the 20 min data. Data having insufficient statistics ( $N(\Delta t) < 1000$ ) have been discarded. Surfactant impurities at the surface render the surface viscous and also suppress the diffusion. The fluctuation dissipation theorem connects the diffusion of particles of radius  $a$  to the friction coefficient

$$f = \frac{k_B T}{D\eta a} \quad (4)$$

where  $k_B$  denotes Boltzmann's constant,  $T = 295$  K is the temperature, and  $\eta = 0.955$  mPa·s is the viscosity of water, which remains unaltered by the addition of salt.<sup>2</sup> The friction coefficient depends on (a) the immersion of the colloidal particles and (b) the surface shear viscosity of the interface that arises due to surfactants. These effects are outlined in detail in ref 7. For a very clean interface, the surface shear viscosity can be neglected and then the friction coefficient rises monotonically with the immersion depth, reaching a value of  $f = 16$  when the colloid is fully immersed into the water, but still touching the

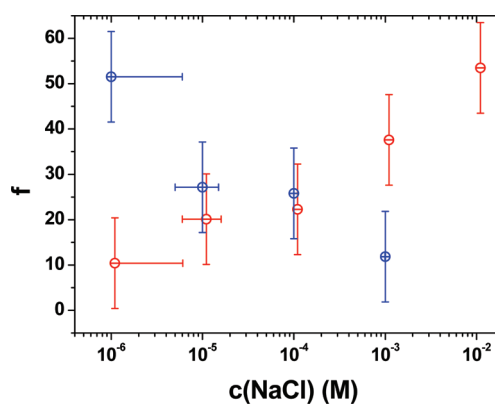


**Figure 3.** Translational drag coefficient  $f$  of positively amino-functionalized ( $\oplus$ ) and negatively carboxylate-functionalized ( $\ominus$ ) charged nanoparticles at the aqueous/air interface as a function of the ionic strength of the sodium chloride solution as derived from the interfacial diffusion of the particles.

interface with its north pole. Upon detaching from the interface, it further rises to  $f = 6\pi$  when the colloid immerses deeper into the water. It is this simple behavior that we use to determine the effect of the charge on the immersion. However, our experimental data does not reach friction coefficients below  $f < 6\pi$  or 16, proving that the surface shear viscosity of surfactants, although it is very low ( $\eta_s \sim 10^{-10}$  N·s/m), cannot be neglected. The friction of the colloidal particle is hence neither 3d nor 2d, but the diffusion coefficient is caused by a coupled 3d–water system and a 2d–surfactant impurity system. Both effects are of similar magnitude. The source of the friction is not only immersion but also controlled by the surfactant impurities. The surfactant impurities are the biggest problem in the evaluation of the data, since there is no real control on the amount of impurities. The diffusion constants determined in the experiments vary from preparation to preparation which we assert to fluctuations in the number of surfactant impurities. The fastest diffusion obtained in the experiment corresponds to the cleanest interface. It is to suppress systematic errors from those impurities that we choose the largest, not the average, mean square displacements in the evaluation of the data. We therefore tried to suppress these systematic errors by choosing the largest mean square displacements among the remaining video sequences. The main error in our measurements results from these surfactant impurities. The error resulting from the analysis of one sample is much smaller. Biasing for the largest mean square displacement minimizes the systematic error. Of course, it increases the statistical error, but the statistical error is smaller.

We assume an uncorrelated diffusion of individual particles which results in a diffusive mean square displacement increasing linearly with the lag time as

$$\langle \Delta x_{\text{diffusivet}}^2 \rangle = 4D\Delta t = 4 \frac{k_B T}{f\eta a} \Delta t \quad (5)$$

We fit the mean square displacement using eq 5 and relate it to the dimensionless friction coefficient  $f$  that measures the response in velocity of the particle to an external force.

## RESULTS AND DISCUSSION

We have measured the dimensionless friction coefficient  $f$  for negative carboxylate-modified particles of radius  $a = 50$  nm and



of amino-functionalized particles of radius  $a = 95$  nm. The particles'  $\zeta$  potentials in ultrapure water were  $\zeta = -29 \pm 2$  mV and  $\zeta = 24 \pm 2$  mV, respectively. This is about half the magnitude of the surface potential of the air/water interface. The friction coefficients of the positive and negative particles have been measured as a function of the ionic strength of a sodium chloride solution. The negative particles remained dispersed up to concentrations in sodium chloride of  $c = 10^{-2}$  M while positive particles started to aggregate for solutions exceeding concentrations of  $c = 10^{-3}$  M. The friction coefficient as a function of salt concentration is depicted in Figure 3. All friction coefficients but those on a bare air/water interface exceed values of  $f > 6\pi$ , indicating that the air/water interface exhibits surface viscous damping on the motion of the beads. Hence, the interface is not free of surfactants. Indeed, the particles being synthesized via emulsion polymerization contain surfactants, partially desorbing from the surface and therefore affecting the diffusion. The slowing down of the diffusion of nanoparticles at interfaces has been observed by other groups.<sup>11</sup> We take it as an indication of the presence of surfactant impurities introduced with the spreading of the particles. Our sodium chloride, however, is free of surfactants and such addition of salt will not affect the surfactant impurity concentration.

Of course, the salt might have an effect on the desorption of surfactants from the colloidal particles. However, surfactant concentrations at the interface are at the detection limit, causing a minute surface shear viscosity of the order of  $\eta_s \sim 10^{-10}$  N·s/m. It is, therefore, clear that the surfactant concentration at the air/water interface is not in thermodynamic equilibrium with the surfactants on the particles. Desorption of surfactants from the colloidal particles for this reason is an irreversible process. Addition of salt to the subphase can cause additional desorption of surfactants, but no readsorption of surfactants on the colloids. It is not possible to explain a speeding up of the diffusion by the addition of salt due to the influence of salt on the desorption rate. This is, however, what we observe for the positively charged particles. The amount of surfactants on the air/water interface cannot decrease. Since surfactant desorption due to increased ion concentration is not the cause of the effect for the positively charged particles, we argue that it is also unlikely for the negatively charged particles. We believe the effect for both positive and negative particles to have the same origin.

Fischer et al.<sup>7</sup> have derived a theory that allows the computation of the dimensionless drag coefficient as a function of the surface shear viscosity of the impurities and as a function of immersion. Using this theory we estimate a surface shear viscosity of the order  $\eta_s \sim 10^{-10}$  N·s/m necessary to explain the data, corresponding to minute amounts of impurities.

The dimensionless friction coefficient increases with ionic strength for the carboxylate-functionalized particles. For the amino-functionalized particles, we observe the opposite behavior and the friction coefficient decreases with ionic strength. According to the theory of Fischer et al.,<sup>7</sup> the friction on a sphere at an interface depends on two major parameters: the surface shear viscosity of the interface, and the depth of immersion of the sphere into the aqueous phase. It is unlikely that the surface shear viscosity of surfactant impurities should in one case increase and in the other case decrease the friction of the nanoparticles. We hence argue that the depth of immersion is a more likely explanation for our measurements. The ionic strength of the solution affects the Debye screening length and hence the electric double layer below the charged particle leading to a decreasing

dipole moment of the particle.<sup>12</sup> The surface potential of the air/water interface, however, is caused by the surface order of the water near the interface. This order decays into the bulk with its own, much shorter, length scale. Electrolyte solutions also affect the surface order;<sup>13</sup> however, the change of surface potential of the air/water interface with ionic strength is weaker than the change of the particles dipole moment. In the simplest picture, we might treat the surface potential of the water as constant while the dipole moment of the particle decreases. The dipole density of the particle is its surface charge density times the Debye length. The dipole density of the air–water surface is its surface potential times the dielectric permittivity. For the negatively charged particles, the dipole densities of the particle and the air/water interface are roughly similar when there are no ions in solution. Addition of ions hence increases the dipole density contrast between the air/water interface and the particle. As a result, the particle is pressed into the interface and diffuses slower. For the positively charged particles, the dipole density contrast is maximal in the absence of ions and decreases when ions are added to the solution. Hence, we propose an expansion of the diffusion constant in the dipole density contrast as

$$D = D_0 - \alpha(\sigma\lambda - \varepsilon\varepsilon_0\psi_w)^2 \quad (6)$$

where  $\sigma$  is the surface charge density of the particle,  $\lambda$  is the Debye length,  $\varepsilon$  and  $\varepsilon_0$  are the relative permittivity of water and the vacuum dielectric constant, and  $\psi_w$  is the surface potential of the air/water interface. The term  $\sigma\lambda/\varepsilon\varepsilon_0$  describes the surface potential of the nanoparticle in the Debye–Hückel approximation for a weak electrolyte. The coefficient  $\alpha$  is a coefficient measuring the effect of the dipole contrast on the diffusion of the particle. In the experiment, we swap the sign of  $\sigma$ , but not the sign of  $\psi_w$ . Addition of salt decreases the Debye length  $\lambda$  in eq 6 and the diffusion constant varies in the opposite way for positive and negative  $\sigma$ . The diffusion constant in eq 6 is invariant under a full charge reversal ( $\sigma \rightarrow -\sigma$ ,  $\psi_w \rightarrow -\psi_w$ ) of both the particle and the surface potential of the interface. It is hence important to consider the nonvanishing surface potential  $\psi_w \sim -50$  mV of the air/water interface to understand the variation of the diffusion constant of small particles with the ionic strength of the solution.

## CONCLUSION

We have shown that the diffusion constant of the interfacial charged particle changes in opposite ways for positive and negative charged particles. The effect can be understood by electrodriving forces on the nanoparticle that push the particle into the aqueous phase. The electrodriving force scales with the contrast in dipole density below the particle and the dipole density of the air/water interface.

## ACKNOWLEDGMENT

We acknowledge support of the German Science Foundation within the Center of Excellence 840: From nanoparticles towards mesotechnology.

## REFERENCES

- (1) Nikolaidis, M. G.; Bausch, A. R.; Hsu, M. F.; Dinsmore, A. D.; Brenner, M. P.; Gray, C.; Weitz, D. A. *Nature* **2002**, *420*, 299.
- (2) Megens, M.; Aizenberg, J. *Nature* **2003**, *242*, 1014.
- (3) Oettel, M.; Dietrich, S. *Langmuir* **2008**, *24*, 1425.

- (4) Exerowa, D. *Kolloid Z. Z. Polym.* **1969**, 232, 703.
- (5) Quincke, G. *Ann. Phys. Chem.* **1861**, 113, 513.
- (6) Dhar, P.; Prasad, V.; Weeks, E.; Bohlein, T.; Fischer, T. M. *J. Phys. Chem. B* **2008**, 112, 9565.
- (7) Fischer, Th. M.; Heinig, P.; Dhar, P. J. *Fluid. Mech.* **2006**, 558, 451.
- (8) Stone H. A. Private communication
- (9) Danov, K. J. *Colloid Interface Sci.* **1995**, 175, 36–1995.
- (10) Sickert, M.; Rondelez, F. *Phys. Rev. Lett.* **2003**, 90, 126104.
- (11) Sickert, M.; Rondelez, F.; Stone, H. A. *EPL* **2007**, 79, 66005.
- (12) Pieranski, P. *Phys. Rev. Lett.* **1980**, 45, 569.
- (13) Gray-Weale, A.; Beattie, J. K. *Phys. Chem. Chem. Phys.* **2009**, 11, 10994.